Silica ash from waste palm fronds used as an eco-friendly, sustainable adsorbent for the Removal of cupper (II)

Fatima A. Al-Qadri*, Raiedhah Alsaiari

Department of Chemistry, College of Science and Art in Sharurah, Najran University,
Kingdome of Saudi Arabia

*Corresponding author's e-mail: fatimaalqadri@gmail.com

Abstract: This study describes the creation of a low-cost silica material using a silicate extract as a precursor. This precursor is made from inexpensive palm frond waste ash through a simple calcination process at 500°C and a green extraction with water. Nitrogen adsorption-desorption, FTIR analyses, and transmission electron microscopy were used to characterize the samples. The surface area of the obtained mesoporous silica ash material was 282 m2/g1, and the pore size was 5.7 nm. For the adsorption of copper ions, an excellent adsorbent was obtained. The maximum copper ion adsorption capacity of this inexpensive silica ash-based adsorbent for removing heavy metal ions Cu(II) from aqueous solutions was 20 mg/g, and the effect of pH, temperature, and time on its adsorption capacity were also investigated. In addition, The adsorption isotherms were fitted using Langmuir and Freundlich models, and the adsorption kinetics were evaluated using pseudo-first-order and pseudo-second-order models

The results demonstrated that the synthesized adsorbent could effectively remove heavy metal ions from aqueous solutions at pH levels ranging from 2 to 5. The adsorption isotherms followed the Langmuir model, and the kinetic data fit the pseudo-second-order mode well. The thermodynamic results Negative values of G° indicate that the adsorption process was spontaneous, and negative values of entropy S° indicate that the state of the adsorbate at the solid/solution interface became less random during the adsorption process. According to the findings, prepared silica from palm waste ash has a high potential for removing heavy contaminating metal ions Cu (II) from aqueous solutions as a low-cost alternative to commercial adsorbents.

Introduction

Water is the most valuable natural resource on the planet, with resources that are among the most important. It is a fundamental component of sustainable growth in all civilizations (Baaloudj et al. 2022). The quality and quantity of water are critical (Gökku et al. 2016). Although water covers more than 71% of the Earth's surface, only 2.5% of it is considered fresh water, and only 0.002% is thought to be accessible to humans (Benrighi et al. 2021).

Water is a limited resource that is constantly being contaminated by dangerous chemicals from Water is a limited resource that is constantly being contaminated by dangerous chemicals from human activities such as agricultural runoff, poor sanitation, and industrialization (Khan et al. 2019, Benrighi et al. 2021). The rapid advancement of science and technology has led to the production of a large number of chemical compounds by the chemical industry (Abdel-Ghani et al. 2007). These hazardous compounds are being released into the environment at an increasing rate, and their concentrations are rising (Boyd et al. 2020). Agricultural waste is one source of water pollution, and waste management strategies are being developed that use waste as a substitute for traditional materials (S.S. Owoeye et al. 2019).

Palm trees are members of the Arecaceae family of evergreen plants. Each date palm tree produces approximately 40 kg of burnable waste per year. Date palm waste is typically burned on farms or disposed of in landfills, causing environmental pollution in date-producing countries. For the long-term utilization of date palm biomass, a variety of physiochemical, thermal, and biochemical technologies are available. Date palm also has a high volatile solid content and a low moisture content. Because of these factors, date palm residues are an excellent biomass resource in date-palm producing countries (Faiad et al. 2022). A date garden has an average economic life of 40 to 50 years, but some can be productive for up to 150 years (Chao et al. 2007). The date palm requires special care during its lifespan. The offshoot

should be removed, and dead or defective fronds should be removed yearly, resulting in approximately 20 kg of waste per year from just one date palm. According to some studies, Saudi Arabia alone generates more than 200,000 tons of date palm biomass each year (Zafar et al. 2021). Date palm wastes include fronds, offshoots, dried frond bases (karab), and date pits. Local farmers say they usually collect and burn this waste. A small portion of the waste is shredded and combined with other biowaste to be used as animal feed, or it is left to decompose naturally and used as fertilizer.

The primary goal of this article is to demonstrate the benefits of processing date palm waste. Researchers have studied and approved the efficiency of date palm waste as an adsorbent in various desalination applications, including the removal of heavy metals such as zinc, cadmium (Hosseinkhani et al. 2014), copper (Al-Ghouti et al. 2010), and lead (Badawi et al. 2021) these heavy metals have polluted natural water resources as a result of the Industrial Revolution, and the WHO has established safe maximum levels of each metal in drinking water. Many researchers have investigated the ability of date palm waste to absorb heavy metals, with a particular focus on the fronds. The fronds are found around the trunk in two spirals, one left-handed and one right-handed, and each mature frond has a rachis, leaflets, and thorns (Kushairi et al. 2019). The aerial part of the oil palm tree, which consists of the petiole and the leaflet, makes up the palm fronds. The petiole, or woody part, accounts for over 70% of the total weight of the frond, while the leaflet weighs less than 30%. Therefore, the proportion of petiole and leaflet portions determined by frond age at harvest is the dominant factor determining the fiber composition of maturing oil palm fronds (Ng, S.K. et al. 2003).

Silicon dioxide (SiO2), also known as silica, is a fundamental material and a valuable inorganic multipurpose chemical compound. In nature, silica is found as quartz, sand, or flint, and it can also be found in agricultural waste like palm ash. These wastes must be properly disposed of, or they will cause a major environmental sustainability issue. For example, according to (Chea Chandra,et al. 2007) the significant amount of this waste presents an opportunity for producing silica for industrial purposes

Even though the production of silica from agricultural waste is lower than that of quartz or sand, it can still be used to meet industrial demands. Adsorption is one of the best approaches because it effectively opens up new avenues for addressing pollution issues. Adsorption is generally preferred for heavy metal ion removal due to its high efficiency, ease of handling, availability of various adsorbents, and cost effectiveness (Kimbrough et al. 1999, and Lin and Juang, 2002).

To that end, the goal of this study is to demonstrate an applied and novel method of using silica ash produced from palm fronds for the purification and removal of heavy metal-polluted water sources, as well as the best treatment of environmental pollution issues by using eco-friendly and more safe methods for human life and economic benefit. FTIR, SEM, and BET were used to characterize the resulting material. The effect of several factors on the preconcentration process was investigated, including shaking time, metal ion concentration, ligand mass, and solution pH.

Materials and Method

Materials and Chemicals
Chemicals
Chemical reagents like oxalic acid and copper nitrate Cu $(NO_3)_2$ were purchased from a chemical reagent company. All of the reagents were analytical grade.

Materials
Many leaching agents, such as HCl, HNO_3, and H_2SO_4, are used in hydrometallurgical extraction techniques to control conditions such as burning temperature and time. However, the majority of these agents pollute the environment. Organic acids such as citric, acetic, and oxalic acids can be appealing leaching agents if the leaching is done at a moderately acidic pH. (Habbache et al. 2009). Extraction and functionalization of silica from palm fronds were obtained locally in this study by collecting palm tree leaves in Sharoura City, Najran, Kingdom of Saudi Arabia.

Instrumentation and characterization
Spectrophotometric measurements were taken using a Perkin--Elmer Lambda 35 spectrophotometer with 1.0 cm^3 quartz cells and a scan speed of 8 nm/sec. The pH was measured with a Jenway 3305 pH meter and a glass-calomel electrode assembly accurate to 0.01 pH units, calibrated using buffer solutions with pH values of 4.0 and 10.0, prepared by dissolving buffer capsules in second-generation de-ionized water. A Jenway 1000 magnetic stirrer was used to stir the solutions. The surface functional groups of the samples were also determined.

Nitrogen (N_2) adsorption-desorption isotherms at 77.5 K were measured using a NOVA 2200e surface area and pore size analyzer (Quantachrome Instruments). The sample's specific surface area was calculated using the BET (Brunauer-Emmett--Teller) method, and the pore size distribution was examined.

Preparation of Silica adsorbent
This study looked into the extraction and functionalization of silica from palm using oxalic acid as a leaching reagent. Local palm fronds and leaves were collected from trees in Sharoura City, Najran, Saudi Arabia. The leaves were cleaned with distilled water, dried for several hours, and then cut into small pieces. The sample was milled into a soft powder using an electric blender, then sieved and stored in a plastic vessel until used in the experiments. Weighing 10 g of palm frond powder (with an average particle size of 75 m) and adding it to a 500 ml beaker contains a specific concentration of oxalic acid solution. The beaker was placed on the hot plate with the magnetic stirrer, and the temperature of the solution was raised to 70°C. The recorded reaction time was 90 minutes. Following the acid leaching process, the palm ash was rinsed with distilled water at room temperature to remove the ash's citric acid content. The materials were dried in the oven at 60°C for two hours before being combusted in the furnace at 800°C for 30 minutes.

Adsorption Isotherm
Batch experiments were conducted with 0.5 g of palm frond silica ash and 100 mL of Cu $(NO_3)_2$ solutions, with initial

Cu (II) concentrations ranging from 100 to 400 mg/L. These were added to various conical flasks, and the adsorption took place for 24 hours at 70°C under normal pH conditions with continuous stirring. The equilibrium adsorption capacities of palm silica ash for Cu (II) were calculated using the following equation:

$$q_{e} = \frac{(c_0 - c_e) \; x \; V}{w} \tag{1}$$

where q_e is the equilibrium adsorption capacity (mg/g); C_0 and Ci are the initial and equilibrium concentrations (mg/L) of the Cu^{2+} solution, respectively; v is the volume of the initial solution (L) used for sorption; and W is the weight of the adsorbent (g).

Kinetic Adsorption
The kinetic reaction occurred and the equilibrium time was determined utilizing 0.5 g of sorbent at 70°C. The adsorption time varied from 30 to 120 min. The kinetics adsorption was estimated by two kinetic models: the pseudo-first-order model and pseudo-second-order model.

Results and Discussion

FTIR spectroscopic studies
The samples' functional group changes were determined using FTIR. The extracted silica FTIR spectra were analyzed according to the steps shown in Fig. 1 (Umeda et al 2010). The main characteristic peaks at 500–1590 and 490–510 cm were assigned to (Si-O-Si), (Si-OH), and (Si-O-Si), respectively (Fernandes et al. 2016). Cu (II) spectrum showed a main characteristic peak at 500 cm, and the formation of a metal oxygen bond caused the peak to appear at around 2360 cm. The presence of metal coordination was confirmed by a strong band at 500 cm, which corresponds to C-O-Cu stretching vibration (Blitz et al. 2007). Additionally, a band at 1650 cm appeared.

Scanning Electron Microscope (SEM)
Palm frond waste samples were fixed on a glass plate with petroleum wax, and a thin film of gold was sprayed for SEM analysis. In the vacuum chamber of the gold depositing machine, gold particles were deposited on the surface of the palm frond. Special conductive liquids were used to make the glass plate conductive as well. Figure 3 shows scanning electron micrographs of palm frond surfaces before they were burned and converted to ash. The results revealed that the surface of the palm frond was rough and undulating (Figure 2a). After calcination, the morphology of palm frond ash was significantly destroyed, and asperities on its surface were almost completely removed (Figure 2b) shows the morphology of silica prepared from pretreated palm fronds and (Figure 2c) shows the) silica ash after adsorption of cu (II).

Nitrogen Adsorption Desorption Analysis
It can be seen in Fig. 3 that the N_2 adsorption isotherm of the functionalized silica gave a hysteresis loop in the range of p/p⁰ values between 0.6 and 0.8, which is associated with capillary
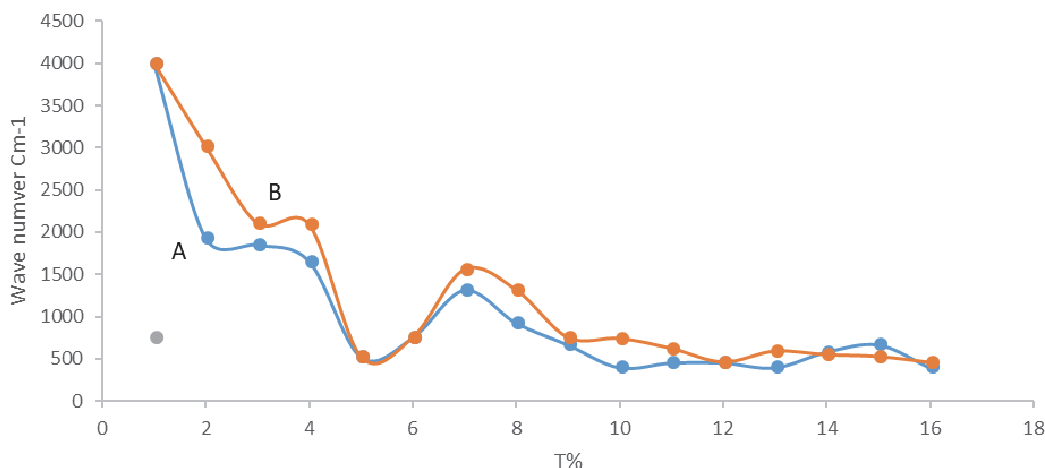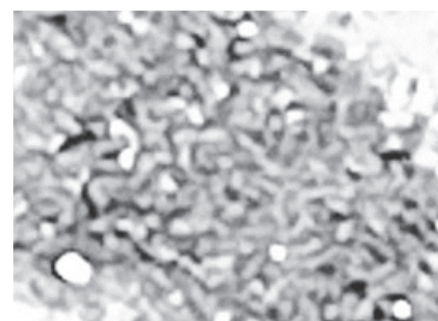

Fig. 1. FTIR of: (A) Activated silica ash free, (B) Cu (II)

(a)   (b)   (c)

Fig. 2. SEM images of (a), palm frond (b) SiO_2 (c) silica ash after adsorption of cu (II)

condensation, a characteristic of mesoporous materials. This demonstrates that the silica is a mesoporous material with pores that are less than 50 nm in diameter, according to the International Union of Pure and Applied Chemistry (Das, et al. 2017) Using BET analysis, the surface area, pore size, and pore volume of the functionalized silica were determined to be 236.36 m^2/g, 0.105 cm^3/g, and 6.18 nm, respectively.

Adsorption Isotherms

At a constant temperature, isotherms show the equilibrium relationship between the amount of adsorbate adsorbed on the adsorbent surface and its concentration in the solution. There are numerous adsorption models in the literature that can be used to fit experimental adsorption data. When the adsorption process reaches an equilibrium state, the adsorption isotherm shows how the adsorption molecules are distributed between the liquid and solid phases. Fitting the isotherm data to different isotherm models is an important step in finding a suitable model that can be used for design purposes (Li et al. 2013). Figure 4 depicts the equilibrium adsorption isotherm of Cu (II) ions onto palm silica ash. It shows a vertical increase at low concentrations and a horizontal plateau at higher concentrations, indicating that the adsorbed amount increases only slightly at higher concentrations.

The adsorption capacity at equilibrium (q_e) increased from 2 mg/g to 6.7 mg/g as the initial Cu (II) concentration increased from 10 to 400 mg/L, as shown in Fig. 4. When the Cu (II) ion concentration was 30 mg/L, the highest value of 7.1 mg/g was obtained, which decreased to 5.9 mg/g at 400 mg/L. The mass transfer driving force increased with initial concentration, resulting in increased adsorption of Cu (II) ions (Syafiqa et al. 2021). Similarly, (KKIU et al. 2013) determined the adsorption effect of neem leaf powder on Cu (II) (NLP). Their findings revealed that the adsorption capacity increased with the initial Cu (II) ion concentration until it reached a maximum, then decreased due to active group saturation. This is consistent with the findings of the current study.

Effect of pH on the adsorption performance of Cu(II)

Figure 5 depicts the effect of solution pH on the adsorption of Cu onto silica ash. Since Cu precipitation is expected when the pH exceeds 5.0, the test is performed in the pH range of 2.0 to 9. As shown in Fig. 5, the adsorption capacity of Cu (II) increased as the pH increased, indicating that the pH value has a significant impact on the adsorption performance of Cu (II). The copper ion adsorption performance on silica ash is poor when pH is less than 4.0.
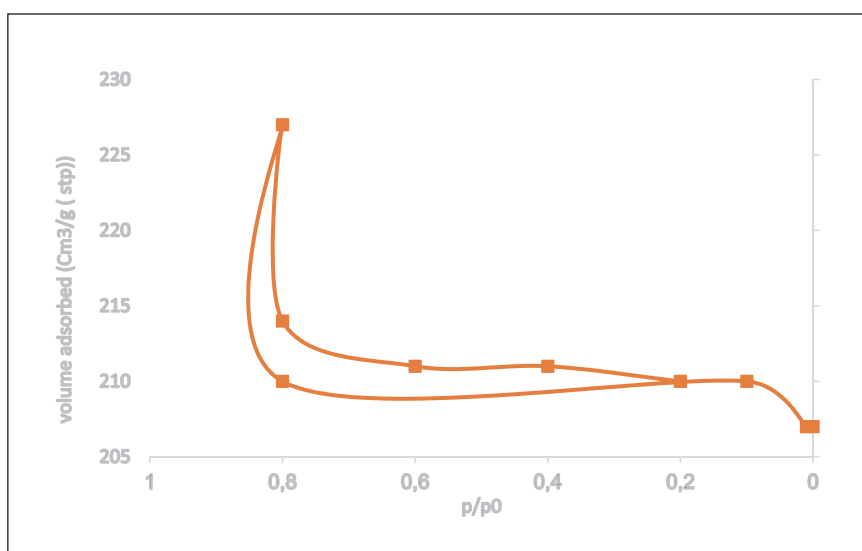

Fig. 3. Adsorption/desorption isotherm of the functionalized silica. Inset: The pore size distribution
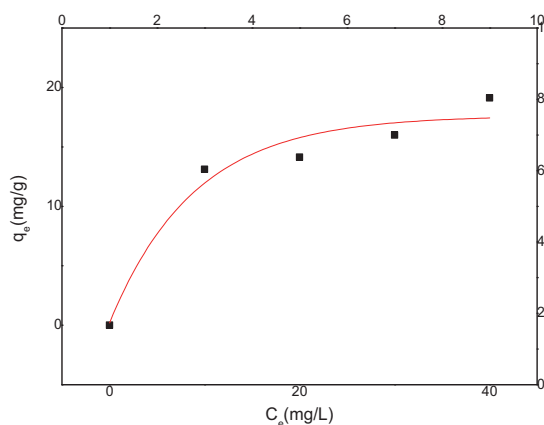

Fig. 4. Effect of initial concentration of Cu (II) ions on adsorption onto silica surface at equilibrium
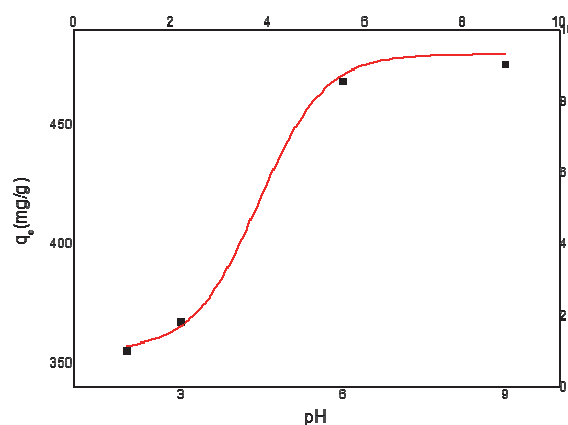

Fig. 5. Effect of pH on Cu adsorption on palm silica ash surface

Effect of mixing speed on adsorption

When the pH of silica ash is 6.0, the maximum amount of Cu adsorption occurs. At low pH values, the water contains a high concentration of hydrogen ions, which can cause the functional group of the adsorbent to be protonated, resulting in the Cu not being completely adsorbed. The hydrogen ions that were originally combined with the functional groups on the mesoporous silica ash material will gradually detach as the pH rises. As the number of adsorption sites that can be used to adsorb Cu increased, so did the adsorption capacity. As a result, the optimal pH value for removing Cu from aqueous solution was found to be between 3 and 6.

Effect of adsorbent dosage on Cu (II) adsorption

The Cu (II) removal percentage increased rapidly as the adsorbent dosage was increased from 1 to 4 g/100 mL, reaching 98% at the 4 g/100 mL dosage (Fig. 7). The removal efficiency gradually reached adsorption equilibrium at a dosage of 2 g/100 mL, and there was no further increase in Cu (II) adsorption with increasing adsorbent dosage. Adsorbent dosage is an important factor in determining an adsorbent's adsorption potential at a given initial concentration. The variation in adsorption capacities at different adsorbent dosages could be attributed primarily to the available adsorption sites. More active sites and surface area of the adsorbent became available for adsorption as the adsorbent dosage increased. The increased adsorbent dosage had no effect on adsorbate uptake once the adsorption reached equilibrium because it added unavailable sites (Elsayed et al. 2020, Mahmudi et al. 2020). Furthermore, while increasing the adsorbent dosage increased the interference of the adsorbent surface among the active groups, the equilibrium concentration of Cu(II) was lower. This was due to the driving force being too low for the adsorbate to diffuse into the adsorbent surface and be adsorbed. These findings are consistent with previous research (Park D, et al. 2008).

Effect of Temperature

Cu (II) ion adsorption onto silica produced from palm ash was studied at 343 K, 353 K, and 373 K with an initial solution concentration of 40 mg/L. As presented in Fig. 8, as the temperature increased from 343 to 373 K, the adsorption of Cu (II) metal ions onto palm silica ash increased from 5.83 mg/g at

353 K to 5.41 mg/g at 373 K. When the adsorbent degraded, it changed the surface chemistry of the sorbent, which increased the availability of active functional groups and decreased heavy metal ion adsorption. Furthermore, as temperatures rose, the bonds shifted, favoring the desorption process (Sharaf and H. Hassan, 2014). The thickness of the boundary layer decreased as the temperature increased because metal ions escaped from the surface into the solution phase, limiting the adsorption capacity (El-Araby, et al. 2017). Similar findings were obtained by (Aksu et al. 2005), who reported that the equilibrium uptake capacity of Cu (II) ions using dried sugar beet pulp as a sorbent decreased from 24.6 to 12.3 mg/g as temperature increased from 25 to 45°C.

Effect of time on adsorption of Cu(II)

Figure 8 shows the relationship between Cu (II) adsorption capacity and time, as well as the relationship between Cu adsorption efficiency and time. As shown in Fig. 8, the adsorption capacity and efficiency of Cu (II) increased over time. The adsorption of Cu by palm silica ash can be divided into two stages: the first reaction stage, which lasted from the beginning to the 30th minute, and the second stage. The first-stage reaction was primarily surface adsorption, which increased adsorption capacity and efficiency while also making the adsorption reaction very fast. The second reaction stage was dominated by gradual adsorption, and
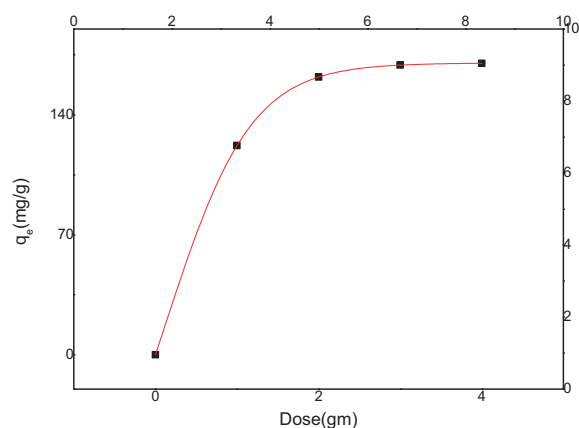
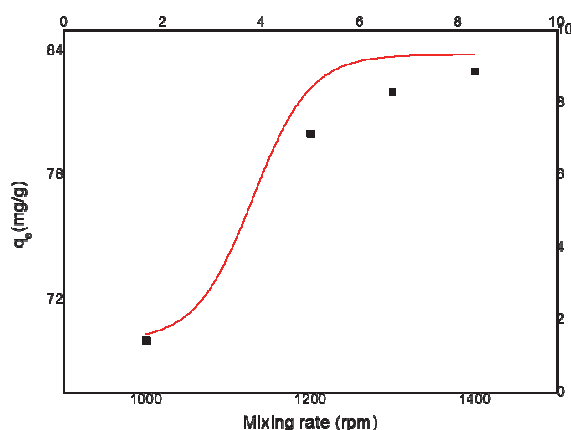**Fig. 7.** Effect of adsorbent dosage of Cu (II) adsorption on palm silica ash surface

Fig. 6. Effect of mixing rate on adsorption of Cu (II) on palm silica ash surface
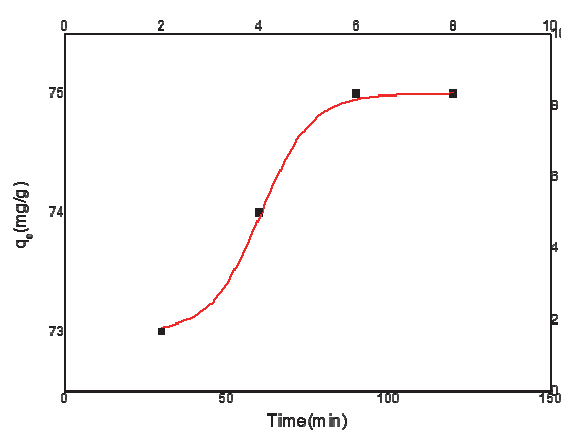
Fig. 8. Effect of contact time on Cu (II) adsorption, 0.25 g/100 mL on palm silica ash surface

the adsorption reaction was relatively slow. It gradually reached equilibrium after 90 to 120 minutes. Because the mesoporous material palm silica ash contains a large number of active sites and has a high mass transfer driving force in the early stages of adsorption, Cu can be easily adsorbed by palm silica ash. However, over time, a large amount of Cu accumulates on the surface of palm silica ash, reducing the number of active sites and impeding Cu movement, resulting in nonlinear adsorption.

Adsorption Isotherms

The adsorption isotherms were obtained using two isotherm models: the Langmuir and Freundlich models. These two models were appropriate for the adsorption process of Cu^{2+} on the silica produced from palm silica ash, as shown in Figs. 9 and 10. The data results are listed in Table 1. The isotherm equations that determined the adsorption process utilized the R_2 values as correlation coefficients. The Langmuir and Freundlich isotherm models were used in this research.

Langmuir Isotherm

The Langmuir isotherm assumes homogeneous adsorption, whereas the Freundlich isotherm is an experimental equation used to depict heterogeneous systems. The results demonstrated that the Langmuir model outperformed the Freundlich model for the adsorption investigated in this study. This suggested that the adsorption process was a homogeneous one. The maximum Cu^{2+} adsorption capacity was 18.51 mg/g, which was higher than or comparable to previously published data (Table 1). When C_e/q_e was plotted against C_e, a straight line with a slope of $1/q_e$ was obtained, as shown in Fig. 9. The results for the adsorption of Cu (II) ions onto silica produced by palm silica ash were well fitted using the Langmuir isotherm, as indicated by a correlation coefficient R2 of 0.97. The slope and intercept were used to calculate the Langmuir constants b and q_{max}, which were related to the adsorption energy and maximum adsorption capacity, respectively. The Langmuir isotherm, which indicates monolayer adsorption, is represented by the following equation (Langmuir et al. 1916):

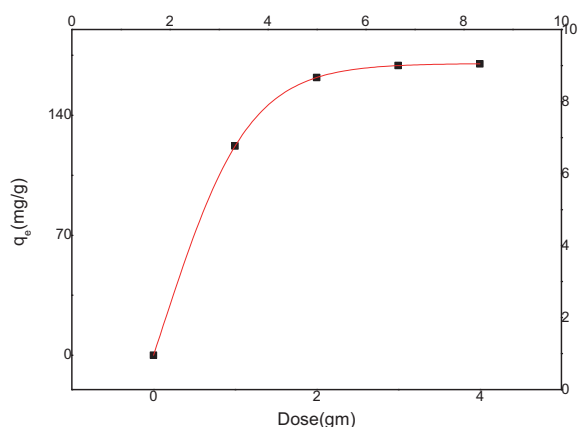$$\frac{c_e}{q_e} = \frac{1}{Q_e.b} + \frac{1}{Q_0}.C_e \qquad (2)$$

Fig. 9. Langmuir isotherm adsorption of Cu (II) onto silica surface

The Langmuir isotherm's essential properties can be expressed in terms of a dimensionless equilibrium parameter (R_L) (Ofomaja and Ho. 2007). The following is the definition of this parameter:

$$R_L = \frac{1}{1 + bC_i} \qquad (3)$$

here C_i is the initial concentration of Cu (II). The RL value indicates that the adsorption is unfavorable: $R_L > 1$; linear: RL = 1; favorable: $0 < RL < 1$; or irreversible: $R_L = 0$. Table 1 lists the Langmuir and Freundlich isotherm model parameters and correlation coefficients for the adsorption of Cu (II) ions on palm silica ash. R_L was found to be 0.0037, 0.00018, 0.00012, and 0.0092. These results emphasized that the Langmuir isotherm was the best at describing the adsorption of Cu (II) ions on the silica produced from palm silica ash. The values of RL were in the range of 0–1, which indicated that the adsorption of Cu (II) metal cations onto the silica produced from palm silica ash was favorable (El-Araby, et al. 2017).

Freundlich Isotherm

The Freundlich isotherm is an experimental model in which qe represents the amount adsorbed per amount of adsorbent at equilibrium (mg/g), Ce represents the equilibrium concentration (mg/L), and Kf and n are Freundlich constants that correspond to adsorption capacity and adsorption intensity, respectively. They are also affected by the adsorbate. The Freundlich equilibrium constants K_f and n are obtained by plotting ln q_e versus log Ce, which results in a straight line with slope n. If n falls between 1 and 10 (1/n is less than 1), they are also influenced by the adsorbate. The Freundlich equilibrium constants $K_{f\ and}$ n are obtained by plotting ln qe versus log Ce, which yields a straight line with slope n. n values within the range of 1–10 are considered favorable for adsorption, where $n > 1$ is the most common and explains the distribution of active centers on the surface or any factor that produces a decrease in adsorbent-adsorbate interaction with increasing surface density. If n is between 1 and 10 (1/n is less than 1), it indicates a physical adsorption of metal ions onto the silica fume ash.

In the present study, *n* was between 1 and 10, which indicated the physical adsorption of metal ions onto the silica fume ash. It had a value of 4.67, and K_F had a value 1.91, as shown in Fig. 10 and Table 1. Freundlich constants K_F and n were calculated using equation (4) and are listed in Table 1. The magnitude of n gives a measure of the favorability of adsorption.

The logarithmic form of the Freundlich model (Freundlich, et al. 1906) is represented by the following equation:

$$\log q_e = \log K_f + \frac{1}{n} \log C_e \qquad (4)$$

Adsorption Kinetics

Several adsorption kinetic models such as the pseudo first-order and pseudo second order models have been used to understand the characteristics and mechanism of adsorption, as well as the rate-limiting step during the adsorption process (Taha, et al. 2017).

The pseudo-first-order model was suggested by (Gupta,et,al. 2001). The linear form of the pseudo-first-order model is expressed as follows:

$$ln(q_e - q_e) = ln\ q_e - k_1 t \qquad (5)$$

where q_e and qt (mg/g) are the amounts of Cu (II) ions adsorbed onto silica extracted from palm waste ash at equilibrium and time t, respectively; and K_1 (min^{-1}) is the rate constant of the pseudo-first-order kinetic model. A straight line was obtained by plotting ln (q_e-q_t) against time. This straight line was used to determine -K_1, correlation coefficient R_2, and the theoretical value of q_e. Although the plot was linear and the calculated value (q_e, calc.) and experimental value (q_e, exp.) were not in agreement with each other, the values of the correlation coefficient for the pseudo-first-order kinetic model were smaller than those of the pseudo-second-order kinetic model. Thus, the adsorption kinetics for the pseudo-first-order kinetic model were poor, as shown in Fig. 11 and Table 2.

Pseudo-second-order reaction
the pseudo-second-order kinetic model of adsorption is dependent on the chemical reactions that occur during the chemisorption process, which involve the exchange of electrons between the adsorbate and adsorbent as a result of valence forces (Ang,et al. 2013). The equilibrium adsorption was evaluated using the following relationship:

$$\frac{t}{q_t} = \frac{1}{k_2 q2_e} + \frac{1}{q_e} \cdot t \qquad (6)$$

where K_2 is the rate constant (g/mg min) of the pseudo-second--order kinetic model. The straight-line plots of t/qt against t

(Fig. 12) were used to determine the values of k_2 and q_e, calc. This model was more likely to predict the behavior over the whole contact time range. As listed in Table 3, the R^2 value for the pseudo-second-order kinetic model was very close to or even equal to unity. Moreover, the calculated equilibrium adsorption capacity values (q_e, calc.) were very close to the experimental (q_e, exp.) values, which indicated that the Cu(II) ion adsorption process onto palm silica ash obeyed the pseudo-second-order model kinetics at all the initial Cu(II) concentrations.

Thermodynamic Parameters
The thermodynamic parameters that determined the process were the changes in the standard enthalpy (H°), standard entropy (S°), and standard free energy (G°) due to the transfer

Fig. 11. Pseudo-first-order plot for adsorption of Cu (II) ions onto silica surface

Table 2. Cu (II) sorption capacities in comparison with those of sorbents in other studies

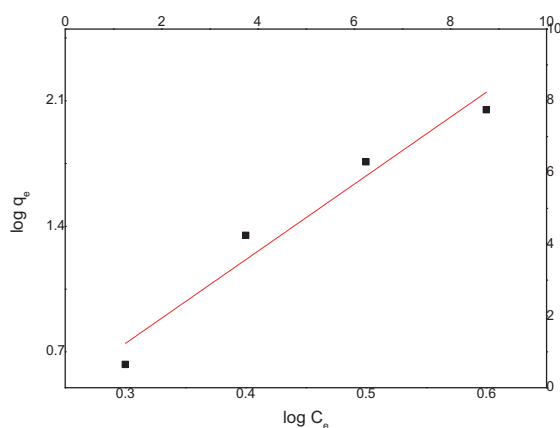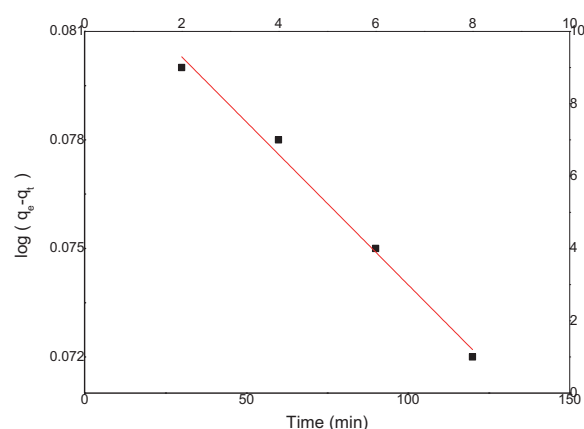| sorbents Adsorbent	Adsorption capacity Cu (II) (mg/g)	Water Research, 32(4) (1998) 1314–1322
Red mud	19.72	Desalination, 229 (2008) 170–180
Soybean straw	5.40	Sep. Purif. Technol., 54 (2007) 187–197

Fig. 10. Freundlich isotherm adsorption of Cu (II) onto silica surface

Table 1. Parameters of Langmuir and Freundlich isotherms for adsorption of Cu (II) ions onto silica surface

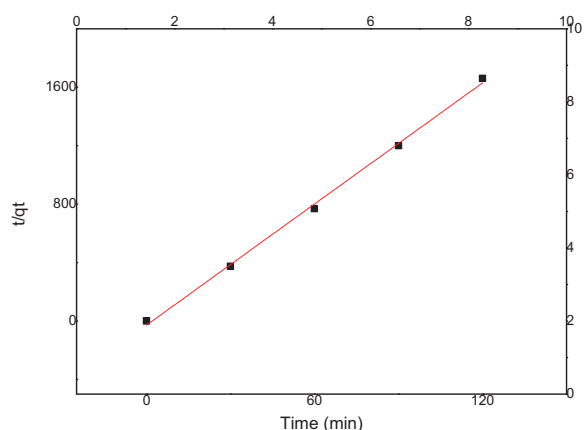| Isotherm model	Evaluated parameters of isotherm		
Langmuir	q_{max} (mg/g)	b (L/mg)	R^2
	18.51	0.56	0.97
Freundlich	n	K_f	R^2
	1.91	0.93	4.67

Fig. 12. Pseudo-second -order plot of adsorption of Cu (II) ions onto silica surface

Table 3. Kinetic parameters and correlation coefficients of two kinetic equations for different initial Cu (II) ion concentrations on silica surface

Metal ion	$q_{e\cdot exp}$ mg/g	First-order kinetic mode			Second-order kinetic mode		
		$q_{e,cal\ (mg/g)}$ mg/g	K1 min	R^2	$q_{e,cal}$ mg/g	K_2 g/gmin	R^2
Cu (II)	7.1	2.11	0.01	0.98	7.23	0.01	0.99

of a unit mole of solute from the solution onto the solid–liquid interface. The values of H° and S° were calculated using the following equations:

$$lnk_d = \Delta\frac{\Delta S°}{R} - \frac{\Delta H°}{RT} \qquad (7)$$

$$\Delta G° = -RTlnK_d \qquad (8)$$

where R is the universal gas constant (8.314 J/(mol.K)); T (K) is the absolute temperature in Kelvin, and Kc is the linear adsorption distribution coefficient, which is defined as follows: Kc = Co/Ce, where Co and Ce (mg/L) are the initial adsorbate concentration and concentration of the adsorbate remaining in the liquid phase at equilibrium, respectively. $\Delta G°$ is the free energy of adsorption, $\Delta H°$ (kJ/mol) is the enthalpy change, and $\Delta S°$ (J/(mol. K)) is the entropy change. The values of H° and S° were calculated from the slope and intercept of the plot for log K versus Temp in Kelvin and it is shown in Figure 13.

The data for the thermodynamic parameters were collected and listed in Table 4. The negative value of $\Delta H°$ shows that the adsorption was exothermic in nature. In addition, the negative value of $\Delta S°$ indicates that the adsorption reaction may be an associative or dissociative mechanism. A negative value for $\Delta S°$ shows that an associative mechanism was involved in the adsorption process. The adsorption in such a case was through the formation of an activated complex between the adsorbate and adsorbent)Aregawi et al.2013). The sign for the entropy $\Delta S°$ value showed that the state of the adsorbate at the solid/solution interface during the adsorption process became less random ($\Delta S° < 0$) or more random ($\Delta S° > 0$) (Tran et al. 2016), as well as a reduction in the degrees of freedom for the Cu (II) ions in the solution. A negative value of $\Delta G°$ indicated that the adsorption process was spontaneous, whereas a positive value for $\Delta G°$ with increasing temperature indicated that the adsorption was non-spontaneous, and that the spontaneous nature of the adsorption was inversely proportional to the temperature.

Conclusion

High-purity silica ash was prepared from palm frond waste ash using oxalic acid as an organic leaching agent instead of inorganic acid. The chemical and structural properties of the silica ash were characterized through various methods, revealing a specific surface area, pore volume, and pore size of 236.36 m²/g, 0.105 cm³/g, and 6.18 nm, respectively.. The adsorption performance of silica ash for removing Cu from aqueous solutions was then investigated Silica ash demonstrated excellent cycle adsorption performance with a dosage of 0.5 g/L, an initial Cu concentration 40 mg/L, an optimum
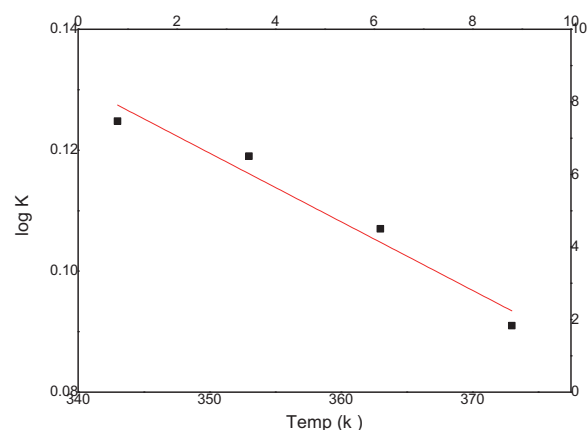
Fig. 13. Effect of temperature on thermodynamic behavior of adsorption of Cu (II) ions onto silica surface

Table 4. Thermodynamic parameters for adsorption of Cu (II) onto silica surface

$\Delta S°$ (J/mol·K)	$\Delta H°$ (kJ/mol)	$\Delta G°$ (kJ/mol)	T (K)
-4290	-93. 3	-7268	343
		-7914	353
		-8006	363
		- 7565	373

pH of 9.0, an equilibrium adsorption time of 120 min, and a chemisorption mechanism following pseudo-second-order kinetics. Cu adsorption capacity increased with temperature, with an ideal reaction temperature of 360°C. Adsorption was governed by both the Langmuir and Freundlich models, with the maximum theoretical adsorption capacity based on the Langmuir model being 18.51 mg/g. The adsorption performance of silica ash mesoporous materials was superior Although only Cu was investigated in this study, future studies are expected to explore the removal of mixed heavy metals from real wastewater. Overall, this study confirms that silica ash from palm fronds is a reliable and low-cost adsorbent for effectively removing Cu from wastewater. Its high surface area also makes it promising for various applications, including catalysts and adsorbents.

Conflict of Interest

All authors approve the final manuscript and declare that there is no conflict of interest.

The data that support the findings of this study are available from the corresponding author upon reasonable request.

Acknowledgments

References

Akin Aksu, A. & C. Deniz, Köksal, (2005). Perceptions and attitudes of tourism students in Turkey. *International Journal Of Contemporary Hospitality Management* 17, 5, pp. 436–447. DOI: 10.1108/09596110510604869

Al-Ghouti, M.A., Li, J., Salamh, Y., Al-Laqtah, N., Walker, G. & Ahmad, M.N.M. (2010). Adsorption mechanisms of removing heavy metals and dyes from aqueous solution using date pits solid adsorbent. *J. Hazard. Mater*. 176, pp. 510–520. DOI: 10.1016/j.jhazmat.2009.11.059.

Ang, X.W., Sethu, V.S., Andresen, J.M., & Sivakumar, M.J.C.T. (2013). Copper (II) ion removal from aqueous solutions using biosorption technology: thermodynamic and SEM–EDX studies. *Clean Technologies and Environmental Policy*, 15(2), pp. 401–407. DOI: 10.1038/s41598-020-73570-7

Aregawi, B.H. & Mengistie, A.A. (2013) Removal of Ni (II) from aqueous solution using leaf, bark and seed of moringa stenopetala adsorbents. *Bulletin of the Chemical Society of Ethiopia*, 27:35. DOI: 10.4314/bcse.v27i1.4

Ayob, S., Othman, N., Altowayti, W.A.H., Khalid, F.S., Bakar, N.A., Tahir, M., & Soedjono, E.S. (2021). A review on adsorption of heavy metals from wood-industrial wastewater by oil palm waste. Journal of Ecological Engineering, 22(3). DOI: 10.12911/22998993/132854

Baaloudj, O., Kenfoud, H., Badawi, A.K., Assadi, A.A., El Jery, A., Assadi, A.A. & Amrane, A. (2022). Bismuth sillenite crystals as recent photocatalysts for water treatment and energy generation: A critical review. *Catalysts*, 12(5), 500. DOI: 10.1016/j.jclepro.2021.129934

Baaloudj, O., Nasrallah, N., Kebir, M., Guedioura, B., Amrane, A., Nguyen-Tri, P., Nanda, S. & Assadi, A.A. (2020). Artificial neural network modeling of cefixime photodegradation by synthesized CoBi2O4 nanoparticles. *Environ. Sci. Pollut. Res*. 28, pp. 15436–15452. DOI: 10.1007/s11356-020-11716-w

Benrighi, Y., Nasrallah, N., Chaabane, T., Sivasankar, V., Darchen, A. & Baaloudj, O. (2021). Photocatalytic performances of ZnCr2O4 nanoparti cles for cephalosporins removal: Structural, optical and electrochemical properties. *Opt. Mater.* 115, 111035.

Blitz, I.P.; Blitz, J.P.; Gun'ko, Z. M.; Sheeran, D.J Functionalized silicas: Structural characteristic and adsorption of Cu(II) and Pb(II). Colloids Surf. A: Physicochem. Eng. Aspects 2007, 307, 83. DOI: 10.1016/j.colsurfa.2007.05.016

Boyd, C.E. (2020). Water Quality Protection. In *Water Quality: An Introduction*, Springer International Publishing: Cham, Switzerland, pp. 379–409, ISBN 978-3-030-23335-8. DOI: 10.1007/978-3-030-23335-8

Chao, C.C.T. & Krueger, R.R. (2007). The date palm (Phoenix dactylifera L.): Overview of biology, uses, and cultivation. *HortScience*, 42, pp. 1077–1082. DOI: 10.21273/HORTSCI.42.5.1077

Chandara, C., Azizli, K.A.M., Ahmad, Z.A., Hashim, S. F.S., & Sakai, E. (2011). Analysis of mineralogical component of palm oil fuel ash with or without unburned carbon. In Advanced materials research (Vol. 173, pp. 7–11). Trans Tech Publications Ltd. DOI: 10.4028/www.scientific.net/AMR.173.7

Das, T., Roy, A., Uyama, H., Roy, P. & Nandi, M. (2017) 2-Hydroxy--naphthyl functionalized mesoporous silica for fluorescence

sensing and removal of aluminum ions, *Dalton Trans*., 46 (22), pp. 7317–7326. DOI: 10.1039/c7dt00369b

El-Araby, H. A., Ibrahim, A.M.M.A., Mangood, A.H., & Adel, A.H. (2017). Sesame husk as adsorbent for copper (II) ions removal from aqueous solution. *Journal of Geoscience and Environment Protection*, 5(07), 109. DOI: 10.4236/gep.2017.57011

Elsayed, A., Osman, D., Attia, S., Ahmed, H., Shoukry, E., Mostafa, Y. & Taman, A. (2020). A Study on the Removal Characteristics of Organic and Inorganic Pollutants from Wastewater by Low Cost Biosorbent. *Egyptian Journal of Chemistry*, 63(4), pp. 1429–1442. DOI: 10.21608/ejchem.2019.15710.1950.

Faiad, A., Alsmari, M., Ahmed, M.M., Bouazizi, M.L., Alzahrani, B. & Alrobei, H. (2022). Date palm tree waste recycling: treatment and processing for potential engineering applications. *Sustainability*, 14(3), 1134. DOI: 10.3390/su14031134

Fernandes, I.J., Calheiro, D.F., Sánchez, A.L., Camacho, A.L.D., de Campos Rocha, T.L.A., Moraes, C.B.A.M. & de Sousa, V.C. (2016). Characterization of Silica Produced from Rice Husk Ash: Comparison of Purification and Processing Methods. *Materials Research*, Vol 20(2), pp. 512–518. DOI: 10.1590/1980-5373-MR-2016-1043

Freundlich, H. (1907). Über die adsorption in lösungen. *Zeitschrift für physikalische Chemie*, 57(1), pp. 385–470 (in Germany). DOI: 10.1515/zpch-1907-5723

Gökku̇, S. Ö. & Yıldız, Y.S. (2016) Application of electro-Fenton process for medical waste sterilization plant wastewater. *Desalin. Water Treat*. 57, pp. 24934–24945. DOI: 10.1080/19443994.2016.1143882

Gupta, V.K., Gupta, M. & Sharma, S. (2001). Process development for the removal of lead and chromium from aqueous solutions using red mud—an aluminium industry waste. Water research, 35(5), 1125–1134., 2001, 35, 1125–1134. DOI: 10.1016/S0043-1354(00)00389-4

Habbache, N., Alane, N., Djerad, S. & Tifouti, L. (2009). Leaching of copper oxide with different acid solutions. *Chemical Engineering Journal* 152, 2–3, 503–508. DOI: 10.1016/j.cej.2009.05.020

Hosseinkhani, H., Euring, M. & Kharazipour, A. (2014). Utilization of Date palm (Phoenix dactylifera L.) Pruning Residues as Raw Material for MDF Manufacturing. J. Mater. Sci. Res. 2014, 4, 46–61. DOI: 10.5539/jmsr.v4n1p46

Kushairi, A., Ong-Abdullah, M., Nambiappan, B., Hishamuddin, E., Bidin, M.N.I.Z., Ghazali, R. & Parveez, G.K.A. (2019). Oil palm economic performance in Malaysia and R&D progress in 2018. *Journal of Oil Palm Research*, 31(2), 165–194. DOI: 10.21894/jopr.2019.0026

Khan, S.T. & Malik, A. (2019). Engineered nanomaterials for water decontamination and purification: From lab to products. *J. Hazard. Mater*. 363, 295–308. DOI: 10.1016/j.jhazmat.2018.09.091

Kimbrough, D.E., Cohen, Y., Winer, A.M., Creelman, L. & Mabuni, C.A. (1999). Critical assessment of chromium in the environment. *Crit. Rev. Environ. Sci. Technol*. 29 (1), pp. 1–46. DOI: 10.1080/10643389991259164

KKIU, Arunakumara Buddhi Charana Walpola, Min-Ho Yoon. (2013) Banana Peel: A Green Solution for Metal Removal from Contaminated WatersI., *Korean J Environ Agric*., Vol. 32, No. 2, pp. 108–116. DOI: 10.1080/10643389991259164

Langmuir, I. (1916) The Constitution and Fundamental Properties of Solids and Liquids. Part I. Solids. *Journal of the American Chemical Society*, 38, 2221–2295. DOI: 10.1021/ja02268a002

Lin, S.H. & Juang, R.S. (2002). Heavy metal removal from water by sorption using surfactant-modified montmorillonite. *J. Hazard. Mater*, 92, pp. 315–326. DOI: 10.1016/S0304-3894(02)00026-2

Mahmudi, M., Arsad, S., Amelia, M.C., Rohman-ingsih, H.A. & Prasetiya, F.S. (2020). An alternative activated carbon from agricultural waste on chromium removal. *Journal of Ecological Engineering*, 21(8), 1–9. DOI: 10.12911/22998993/127431

Namasivayam, C., Prabha, D. & Kumutha, M. (1998). Removal of direct red and acid brilliant blue by adsorption on to banana pith. *Bioresource Technol*. 64, pp. 77–79. DOI: 10.1016/S0960-8524(97)86722-3

Owoeye, S. S., Toludare, T.S., Isinkaye, O.E. & Kingsley, U. (2019). Influence of waste glasses on the physico-mechanical behavior of porcelain ceramics. *Boletín de la Sociedad Española de Cerámica y Vidrio*, 58(2), 77–84. DOI: 10.1016/j.bsecv.2018.07.002

Park, D., Lim, S.R., Yun, Y.S. & Park, J.M. (2008). Development of a new Cr(VI)-biosorbent from agricultural biowaste. *Bioresource Technol*. 1 99: 8810–8818. DOI: 10.1016/j.biortech.2008.04.042

Sharaf, G. & Hassan, H. (2014). Removal of copper ions from aqueous solution using silica derived from rice straw: comparison with activated charcoal. *International Journal of Environmental Science and Technology*. DOI: 10.1007/s13762-013-0343-8

Taha, A.A., Ahmed, A.M., Abdel Rahman, H.H., Abouzeid, F.M. & Abdel Maksoud, M.O. (2017).Removal of nickel ions by adsorption on nano-bentonite: Equilibrium, kinetics, and thermodynamics. *J. Dispers. Sci. Technol.*, 38, 757–767. DOI: 10.1080/01932691.2016.1194211

Umeda, J. & Kondoh, K. (2010). High-purification of amorphous silica originated from rice husks by combination of polysaccharide hydrolysis and metallic impurities removal. *Industrial Crops and Products*, 32 (3): 539–544. DOI: 10.1016/j.indcrop.2010.07.002

Zhu, W., Wang, J., Wu, D., Li, X., Luo, Y Han, C. & He, S. (2017). Investigating the heavy metal adsorption of mesoporous silica materials prepared by microwave synthesis. *Nanoscale research letters*, 12(1), 1–9. A.A. DOI: 10.1186/s11671-017-2070-4

Zuraidah, Y., Haniff, M.H. & Zulkifli, H. (2017). Does soil compaction affect oil palm standing biomass. *Journal of Oil Palm Research*, *Kajang*, 29(3), 352–357. DOI: 10.21894/jopr.2017.2903.07